

# Synthesis of Ferrocenethiols Containing Oligo(phenylenevinylene) Bridges and Their Characterization on Gold Electrodes

Stephen P. Dudek, Hadley D. Sikes, and Christopher E. D. Chidsey\*

Contribution from the Department of Chemistry, Stanford University, Stanford, California 94305-5080

Received December 27, 2000. Revised Manuscript Received May 18, 2001

**Abstract:** Ferrocene-terminated oligo(phenylenevinylene) (OPV) methyl thiols have been prepared by orthogonal coupling of phenylene monomers. Ethoxy substituents on the phenyl rings improve the solubility of OPV, enabling the synthesis of longer oligomers. Self-assembled monolayers containing a mixture of a ferrocene OPV methyl thiol and a diluent alkanethiol were deposited on gold. A cyclic voltammetric study of monolayers containing oligomers of the same length with and without ethoxy solubilizing groups reveals that both solubilized and unsolubilized oligomers form well-packed self-assembled monolayers. Changing the position of the solubilizing groups on an oligomer chain does not preclude packing of the oligomer in the monolayer. Conventional chronoamperometry, which can be used to measure rate constants up to  $\sim 10^4 \text{ s}^{-1}$ , is too slow to measure the electron-transfer rate through these oligomers over distances up to 35 Å. OPV bridges are expected to be highly conjugated unlike oligo(phenyleneethynylene) bridges, which may be only partially conjugated because of rotation of the phenyl rings about the ethynylene bonds. Because of its high conjugation, OPV may prove useful as a molecular wire.

## Introduction

Formation of self-assembled monolayers containing highly  $\pi$ -conjugated organic oligomers would facilitate the investigation of interfacial electron transfer and the design of biosensors<sup>1</sup> and molecular devices.<sup>2</sup> To this end, several research groups have studied oligo(phenyleneethynylene) (OPE) thiols deposited as self-assembled monolayers on gold.<sup>3–5</sup> Ferrocene-terminated OPE thiols transport electrons faster than their ferrocene alkanethiol counterparts; the distance dependence of the log of the rate constant,  $\beta = -d \ln k_{\text{et}}/dx$ , was found to be 0.4–0.6 Å<sup>-1</sup> for OPE<sup>3,4</sup> as compared to  $\sim 1.0 \text{ Å}^{-1}$  for alkane bridges.<sup>6–8</sup> Although OPE can transport electrons faster than alkanes, OPE may not be optimally  $\pi$ -conjugated because energetically feasible rotations of adjacent phenyl rings around the intervening ethynylene bonds can decrease the conjugation of the  $\pi$ -system.<sup>3,9</sup> In contrast, oligo(phenylenevinylene) (OPV) is composed of coplanar phenyl groups linked by vinylene bonds around which the phenyl groups have a higher barrier of rotation than

in the OPE system.<sup>10</sup> Thus, OPV could be expected to transport electrons even faster than OPE.

We present the synthesis of ferrocene OPV methyl thiols and the characterization of the resulting monolayers. On the basis of a synthesis of OPV previously reported by Maddux et al.,<sup>11</sup> we have developed asymmetric oligomers with ferrocene on one end and methyl thiol on the other end to make the oligomers electroactive and capable of self-assembly on gold. We have chosen to terminate the OPV oligomers with methyl thiol because aryl methyl thiols are more readily synthesized and more stable in solution than aryl thiols. Although the additional methylene is expected to reduce electronic coupling, this reduction should be constant for all the oligomers. Because rigid oligomers such as OPV tend to have poor solubility at long oligomer lengths, we have attached solubilizing groups to the phenyl rings. By varying the number and position of solubilizing groups, we have explored their effect on monolayer packing. We find that both unsolubilized and solubilized ferrocene OPV methyl thiols form well-behaved self-assembled monolayers. Switching the position of solubilizing groups on an oligomer to a phenyl position closer to the gold surface does not severely impair the packing of the oligomer in the mixed monolayer. For even the longest oligomer length so far synthesized (35 Å), we find that conventional chronoamperometric methods on a planar macroscopic electrode are unable to determine the rate constants of electron transfer, presumably because the rate constants exceed the  $\sim 10^4 \text{ s}^{-1}$  limit of the method. The rate constants for the monolayers reported here have recently been

\* To whom correspondence should be addressed: chidsey@stanford.edu.

(1) Willner, I.; HelegShabtai, V.; Blonder, R.; Katz, E.; Tao, G. L. *J. Am. Chem. Soc.* **1996**, *118*, 10321.

(2) Bumm, L. A.; Arnold, J. J.; Cygan, M. T.; Dunbar, T. D.; Burgin, T. P.; Jones, L.; Allara, D. L.; Tour, J. M.; Weiss, P. S. *Science* **1996**, *271*, 1705.

(3) Sachs, S. B.; Dudek, S. P.; Hsung, R. P.; Sita, L. R.; Smalley, J. F.; Newton, M. D.; Feldberg, S. W.; Chidsey, C. E. D. *J. Am. Chem. Soc.* **1997**, *119*, 10563.

(4) Creager, S.; Yu, C. J.; Bamdad, C.; O'Conner, S.; MacLean, T.; Lam, E.; Chong, Y.; Olsen, G. T.; Luo, J. Y.; Gozin, M.; Kayyem, J. F. *J. Am. Chem. Soc.* **1999**, *121*, 1059.

(5) Cygan, M. T.; Dunbar, T. D.; Arnold, J. J.; Bumm, L. A.; Shedlock, N. F.; Burgin, T. P.; Jones, L.; Allara, D. L.; Tour, J. M.; Weiss, P. S. *J. Am. Chem. Soc.* **1998**, *120*, 2721.

(6) Smalley, J. F.; Feldberg, S. W.; Chidsey, C. E. D.; Linford, M. R.; Newton, M. D.; Liu, Y. P. *J. Phys. Chem.* **1995**, *99*, 13141.

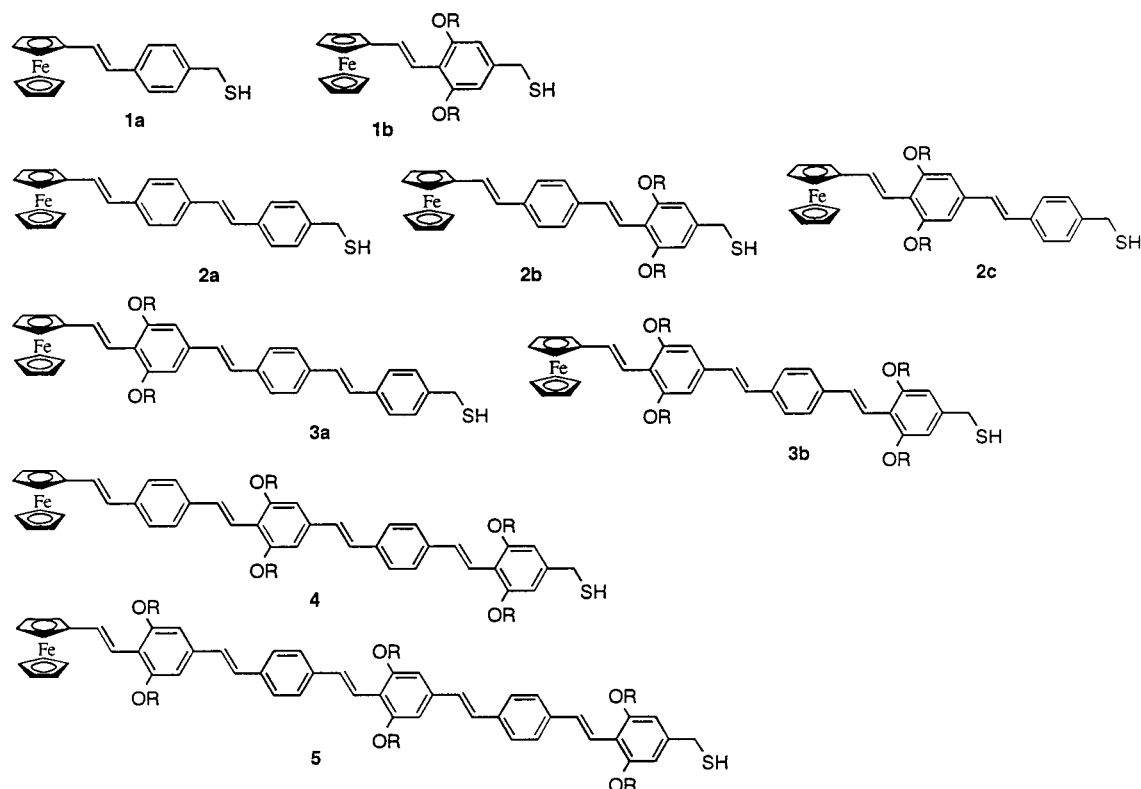
(7) Weber, K.; Hockett, L.; Creager, S. *J. Phys. Chem. B* **1997**, *101*, 8286.

(8) Finklea, H. O.; Hanshew, D. D. *J. Am. Chem. Soc.* **1992**, *114*, 3173.

(9) Okuyama, K.; Hasegawa, T.; Ito, M.; Mikami, N. *J. Phys. Chem.* **1984**, *88*, 1711.

(10) Bock, C. W.; Trachtman, M.; George, P. *Chem. Phys.* **1985**, *93*, 431.

(11) Maddux, T.; Li, W. J.; Yu, L. P. *J. Am. Chem. Soc.* **1997**, *119*, 844. Wong, M. S.; Li, Z. H.; Shek, M. F.; Chow, K. H.; Tao, Y.; Diorio, M. *J. Mater. Chem.* **2000**, *10*, 1805. Davis, W. B.; Svec, W. A.; Ratner, M. A.; Wasielewski, M. R. *Nature* **1998**, *396*, 60. Eckert, J. F.; Nicoud, J. F.; Nierengarten, J. F.; Liu, S. G.; Echegoyen, L.; Barigelli, F.; Armaroli, N.; Ouali, L.; Krasnikov, V.; Hadziioannou, G. *J. Am. Chem. Soc.* **2000**, *122*, 7467.

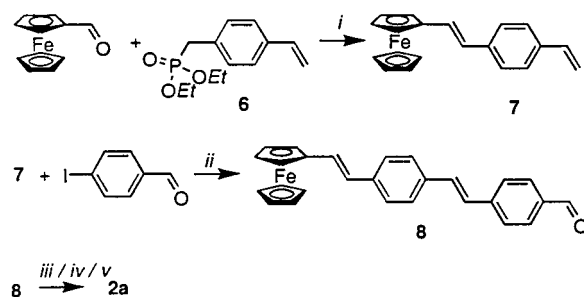
**Chart 1.** Ferrocene OPV Methyl Thiols (R = C<sub>2</sub>H<sub>5</sub>)

measured by the indirect laser-induced temperature jump method (a potentiometric method); all exceed  $10^5 \text{ s}^{-1}$ .<sup>25</sup>

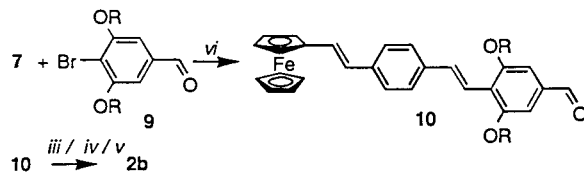
## Results and Discussion

**Ferrocene-Terminated OPV Methyl Thiols.** Chart 1 shows the nine ferrocene-terminated OPV methyl thiols of five oligomer lengths that we have synthesized. These oligomers are constructed from either vinylferrocene or ferrocenecarboxaldehyde to which is added one phenylene monomer per coupling reaction. Vinyl connections are made by alternating Heck coupling of *p*-halobenzaldehydes to terminal styrenes and Horner–Wadsworth–Emmons coupling of *p*-vinylbenzylphosphonates to terminal benzaldehydes. These alternating, orthogonal couplings expedite oligomer-chain extension by obviating the need for protecting groups. To cap the oligomer chain with methyl thiol, we reduce the chain's terminal benzaldehyde, convert the benzyl alcohol to a benzyl thioacetate, and reduce the benzyl thioacetate to the benzyl thiol, which is described in the following as an aryl methyl thiol. As an example, the synthesis of **2a**, a ferrocene OPV dimer methyl thiol, is outlined in Scheme 1.

Some solubilization of oligo(phenylenevinylene) is needed for long chains because synthetic intermediates longer than two unsolubilized phenylenevinylene units are not sufficiently soluble for further transformation in common organic solvents. 3,5-Diethoxy substitution on the phenyl rings is one way to increase the solubility of OPV. The commercial availability of 4-bromo-3,5-dihydroxybenzoic acid, a precursor of benzaldehyde **9**, permits convenient attachment of 3,5-diethoxy groups to the phenylene adjoining the methyl thiol on an oligomer and to every alternate phenylene prior to this terminal phenylene. As an example, Scheme 2 outlines the synthesis of **2b**, a ferrocene OPV dimer methyl thiol with one set of solubilizing groups. To test the effect of solubilizing groups on oligomer packing in the self-assembled monolayer, we desired more

**Scheme 1.** Synthesis of **2a**<sup>a</sup>

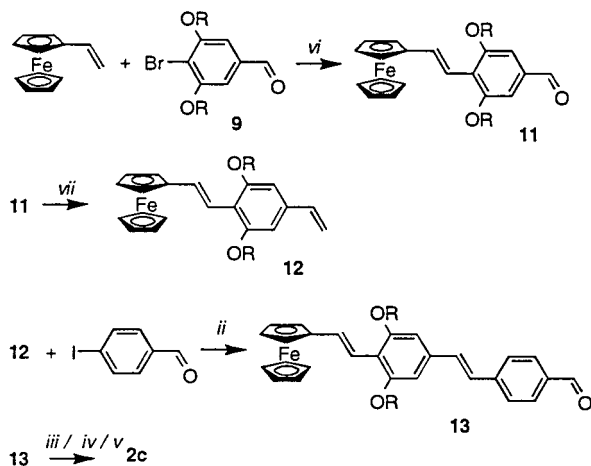
<sup>a</sup> Reaction Conditions: (i) NaH, DME. (ii) Palladacycle, NaOAc, DMA. (iii) NaBH<sub>4</sub>, THF. (iv) DEAD, PPh<sub>3</sub>, AcSH, THF. (v) LiAlH<sub>4</sub>, THF.

**Scheme 2.** Synthesis of **2b** (R = C<sub>2</sub>H<sub>5</sub>)<sup>a</sup>

<sup>a</sup> Reaction Conditions: (iii) NaBH<sub>4</sub>, THF. (iv) DEAD, PPh<sub>3</sub>, AcSH, THF. (v) LiAlH<sub>4</sub>, THF. (vi) Pd(OAc)<sub>2</sub>, P(*o*-tolyl)<sub>3</sub>, NBu<sub>3</sub>, DMA.

flexibility in placing solubilizing groups. Wittig conversion of an oligomer's terminal benzaldehyde to a styrene permits the placement of solubilizing groups on any and all of an oligomer's phenylenes. This Wittig conversion is used in the synthesis of **2c** (Scheme 3). With this synthetic strategy, we developed sets of oligomers of the same length but having differently positioned solubilizing groups.

<sup>1</sup>H NMR spectroscopy of the ferrocene OPV methyl thioacetates indicates one doublet for each vinylic proton, which suggests that each oligomer has a single diastereomeric conformation and is not a mixture of *cis* and *trans* isomers. The

**Scheme 3.** Synthesis of **2c** (R = C<sub>2</sub>H<sub>5</sub>)<sup>a</sup>

<sup>a</sup> Reaction Conditions: (ii) palladacycle, NaOAc, DMA, (iii) NaBH<sub>4</sub>, THF, (iv) DEAD, PPh<sub>3</sub>, AcSH, THF, (v) LiAlH<sub>4</sub>, THF, (vi) Pd(OAc)<sub>2</sub>, P(o-tolyl)<sub>3</sub>, NBu<sub>3</sub>, DMA, (vii) *n*-BuLi, PPh<sub>3</sub>CH<sub>3</sub>Br, THF.

**Table 1.** Long-Wavelength Absorption Maximums of Ferrocene-Terminated OPV Methyl Thioacetates Measured in CH<sub>2</sub>Cl<sub>2</sub>

compd	$\lambda_{\max}$ (nm)	$E_{\max}$ (L·mol <sup>-1</sup> · cm <sup>-1</sup> )	compd	$\lambda_{\max}$ (nm)	$E_{\max}$ (L·mol <sup>-1</sup> · cm <sup>-1</sup> )
<b>1a</b>	313 ± 2	3 ± 2 × 10 <sup>4</sup>	<b>3a</b>	387 ± 2	9 ± 3 × 10 <sup>4</sup>
<b>1b</b>	322 ± 2	4 ± 2 × 10 <sup>4</sup>	<b>3b</b>	390 ± 2	7 ± 3 × 10 <sup>4</sup>
<b>2a</b>	357 ± 2	6 ± 2 × 10 <sup>4</sup>	<b>4</b>	416 ± 2	3 ± 1 × 10 <sup>5</sup>
<b>2b</b>	366 ± 2	8 ± 3 × 10 <sup>4</sup>	<b>5</b>	426 ± 2	4 ± 1 × 10 <sup>5</sup>
<b>2c</b>	366 ± 2	5 ± 3 × 10 <sup>4</sup>			

coupling constants found for the vinylic bonds of the oligomers are 16.6 ± 0.6 Hz, which are above the 6–14-Hz range expected for *cis* coupling and within the 11–18-Hz range expected for *trans* coupling.<sup>12</sup> The presence of only one vinylic doublet for each monomer unit and the magnitude of their coupling constants indicate that the vinyl bonds of the oligomers are exclusively in the *trans* geometry.<sup>13</sup>

**Properties of Protected Ferrocene-Terminated OPV Methyl Thioacetates.** UV/visible spectroscopy provides a probe of the spacing between the HOMO and LUMO of conjugated molecules, a quantity relevant to their ability to promote electron tunneling. We acquired spectra of the thioacetate-protected oligomers because these protected oligomers are more stable than their deprotected thiol counterparts and the acetyl group is not expected to perturb significantly the absorbance spectrum. The conjugated phenylenevinylene portions of the oligomers absorb strongly between 300 and 450 nm (Table 1). The peak position of the absorption,  $\lambda_{\max}$ , shifts bathochromically with longer chain length and additional solubilizing groups; the extinction coefficient of the absorption likewise increases with longer oligomer length. These trends are similar to those reported for symmetric oligomers of phenylenevinylene. Up to

(12) Dean, J. A., Ed. *Lange's Handbook of Chemistry*, 14th ed.; McGraw-Hill: New York, 1992; Table 7.46.

(13) <sup>1</sup>H NMR spectroscopy does not indicate whether the vinylene groups adopt *cisoid* or *transoid* configurations about the phenylene groups. The rotation of the vinyl group around the single carbon–carbon bond in styrene is calculated to have a barrier of 3.1 kcal/mol,<sup>10</sup> suggesting that dissolved oligo(phenylenevinylene), although planar, can interconvert between *cisoid* and *transoid* geometries about the phenylenes in solution at room temperature. In the solid state (either in a crystal or as part of a monolayer), OPV may adopt exclusively one geometry. The specific *cisoid* or *transoid* geometry of the ferrocene-terminated OPVs is not expected to affect dramatically the rates of electron transfer through the OPV chain. (Marshall Newton, private communication).

the length of the pentamer,  $\lambda_{\max}$  for the ferrocene-terminated OPVs continues to shift to higher wavelength, suggesting that the limit of convergence for this series is greater than five. Maddux and co-workers found empirically that this limit is reached at  $n = 8$  for asymmetric, aldehyde-terminated OPV.<sup>11</sup> For symmetric, hydrogen-terminated OPV, Meier and Stalmach found this limit to be reached at  $n = 11$ .<sup>14</sup>

When excited at  $\lambda_{\max}$ , ferrocene-terminated OPVs emit more weakly than a laser dye with a similar  $\lambda_{\max}$  probably because of quenching of the OPV excited state by ferrocene.<sup>15</sup> For example, commercially available Coumarin 540A<sup>16</sup> ( $\lambda_{\max} = 425$  nm) emits 40 times more efficiently per absorbed photon than thioacetate-protected **5** ( $\lambda_{\max} = 426$  nm). The shorter OPV chains show even weaker emission efficiencies.

Cyclic voltammograms (CVs) of solutions of protected ferrocene OPV methyl thioacetates in contact with gold electrodes exhibit peak shapes and peak splittings characteristic of freely diffusing redox species in contact with an electrode.<sup>17</sup> For example, we studied **2b** in an acetonitrile solution of 0.1 M tetrabutylammonium hexafluorophosphate. This solution was placed in contact with a gold electrode coated with a passivating monolayer of pentanethiol to prevent contamination of the electrode surface. For this system, the potential difference between the peaks of the oxidative and reductive waves,  $\Delta E_{p-p}$ , is 65 mV at a scan rate of 50 mV/s which is close to the 60-mV  $\Delta E_{p-p}$  expected for diffusive redox species in contact with an electrode.<sup>17</sup>

**Properties of Monolayers Containing Ferrocene-Terminated OPV Methyl Thiols.** Deprotected as free thiols, ferrocene OPV methyl thiols absorb on gold. CVs of monolayers deposited from solutions of only the ferrocene-terminated OPV methyl thiol show large coverages of ferrocene. The CVs, however, are broad and exhibit peak splitting. The number of electroactive molecules in a monolayer is calculated by integrating the peak in the CV above the baseline and dividing by scan rate, electrode area, and elementary charge. The coverage values determined from the oxidation and reduction peaks are averaged. A CV of a monolayer deposited from a 0.3 mM chloroform solution of **4** shows a coverage of 83% of the density of the  $\sqrt{3} \times \sqrt{3} R$  30° alkanethiol monolayer on Au(111).<sup>18</sup> At a scan rate of 100 mV/s, the peak splitting is 39 mV, which suggests structural hysteresis of the monolayer. The peak of the CV has a full width at half-maximum (fwhm) of 173 mV, which is much larger than the 90 mV fwhm predicted for identical, noninteracting tethered redox groups.<sup>17,19</sup> The peak broadening suggests either interaction between the ferrocene sites or inhomogeneity of those sites at high surface coverages.

To isolate the adsorbed ferrocenes and improve the uniformity of these ferrocene sites, we codeposited ferrocene OPV methyl thiols with alkanethiols as diluents.<sup>18</sup> Figure 1 shows CVs of monolayers deposited from 0.3 mM solutions of 30 mol % **2b** and 70 mol % pentanethiol, decanethiol, or hexadecanethiol. The coverage of **2b** with a pentanethiol diluent is much higher than the coverage of **2b** with a decanethiol diluent. Pentanethiol absorbs less avidly than decanethiol on the surface.

(14) Stalmach, U.; Kolshorn, H.; Brehm, I.; Meier, H. *Liebigs Ann. Chem.* **1996**, 1449.

(15) Giasson, R.; Lee, E. J.; Zhao, X.; Wrighton, M. S. *J. Phys. Chem.* **1993**, *97*, 2596–2601. Guldi, D. M.; Maggini, M.; Scorrano, G.; Prato, M. *J. Am. Chem. Soc.* **1997**, *119*, 974–980.

(16) Exciton, Inc., P.O. Box 31126, Overlook Station, Dayton, OH 45431. (17) Bard, A. J.; Faulkner, L. R. *Electrochemical Methods*, 2nd ed.; John Wiley & Sons: New York, 2001.

(18) Chidsey, C. E. D.; Bertozzi, C. R.; Putvinski, T. M.; Mujcsa, A. M. *J. Am. Chem. Soc.* **1990**, *112*, 4301.

(19) Smith, C. P.; White, H. S. *Anal. Chem.* **1992**, *64*, 2398.

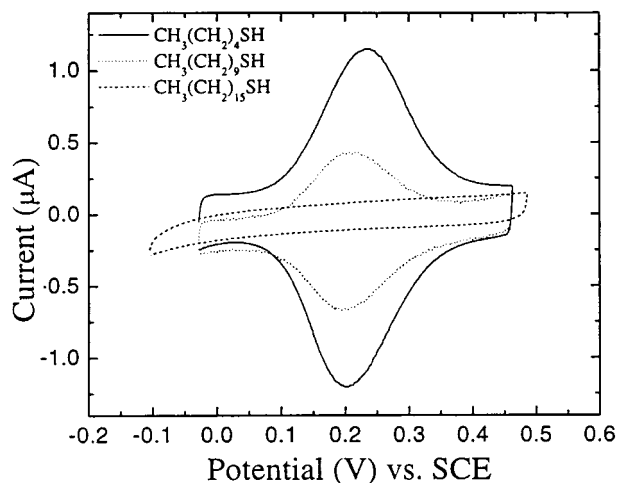


**Figure 1.** Cyclic voltammograms of mixed monolayers deposited from solutions of 30 mol % **2b** and 70 mol % pentanethiol, decanethiol, and hexadecanethiol. The scan rate was 100 mV/s. Double-layer capacitances, full width at half-maximums, and fractional surface coverages of the electroactive species derived from the CVs are (pentanethiol) 6.1  $\mu\text{F}/\text{cm}^2$ , 114 mV, 7.2%; (decanethiol) 3.0  $\mu\text{F}/\text{cm}^2$ , 108 mV, 3%; (hexadecanethiol) 2.0  $\mu\text{F}/\text{cm}^2$ , - 0%. Potentials were measured vs a Ag/AgClO<sub>4</sub> reference electrode but have been converted to potentials vs SCE.

The capacitance of the monolayer formed from **2b** and pentanethiol is twice as high as the capacitance of the monolayer formed from **2b** and decanethiol. This increase can be attributed to the inverse proportionality of alkanethiol length and capacitance as found for pure alkanethiol monolayers.<sup>20</sup> With a hexadecanethiol diluent, the ferrocene redox peak disappears. Either the longer hexadecanethiol diluent precludes deposition of the shorter **2b** or diluents longer than the codeposited oligomer prevent ferrocene oxidation by blocking ion permeation to the buried ferrocene.<sup>21</sup> On the basis of this study, the length of the alkane thiol diluent in mixed-monolayer depositions was chosen to be slightly shorter than the ferrocene OPV methyl thiol so that the ferrocene can be positioned in the electrolyte above the alkane monolayer surface.

Figure 2a shows a cyclic voltammogram of a monolayer formed by soaking a gold substrate in a solution of 30 mol % **2a** and 70 mol % decanethiol. The lack of peak splitting indicates that the electron-transfer rate across the monolayer is fast compared to the 100 mV/s scan rate. The 112 mV fwhm of the peak agrees fairly well with the 90 mV fwhm predicted for an ideal noninteracting tethered redox group.<sup>17</sup> This agreement indicates that the ferrocene groups are nearly identical and are outside the interfacial charge double layer; if the ferrocenes were within the charge double layer, the CV would show much greater peak broadening.<sup>19</sup> The fractional surface coverage of ferrocene thiol in this monolayer is 11% of the density of the  $\sqrt{3} \times \sqrt{3} R 30^\circ$  alkanethiol layer on Au(111).<sup>18</sup> The background charging current in Figure 2a gives an interfacial capacitance of 1.9  $\mu\text{F}/\text{cm}^2$ ; from this value, we calculate<sup>22</sup> an effective dielectric thickness of 11 Å, placing the ferrocene groups at least 11 Å from the gold surface.

At low coverages of ferrocene OPV methyl thiol, the ellipsometric thickness of the mixed monolayers corresponds

(20) Chidsey, C. E. D.; Loiacono, D. N. *Langmuir* **1990**, *6*, 682.

(21) Creager, S. E.; Rowe, G. K. *J. Electroanal. Chem.* **1997**, *420*, 291.

(22) If the monolayer is treated as an ideal capacitor, Helmholtz theory predicts that  $d = (\epsilon\epsilon_0/C)$ , where  $d$  is the thickness of the dielectric medium (the monolayer),  $\epsilon$  is the dielectric constant of the monolayer,  $\epsilon_0$  is the permittivity of free space, and  $C$  is the capacitance of the monolayer per unit area.<sup>20</sup>

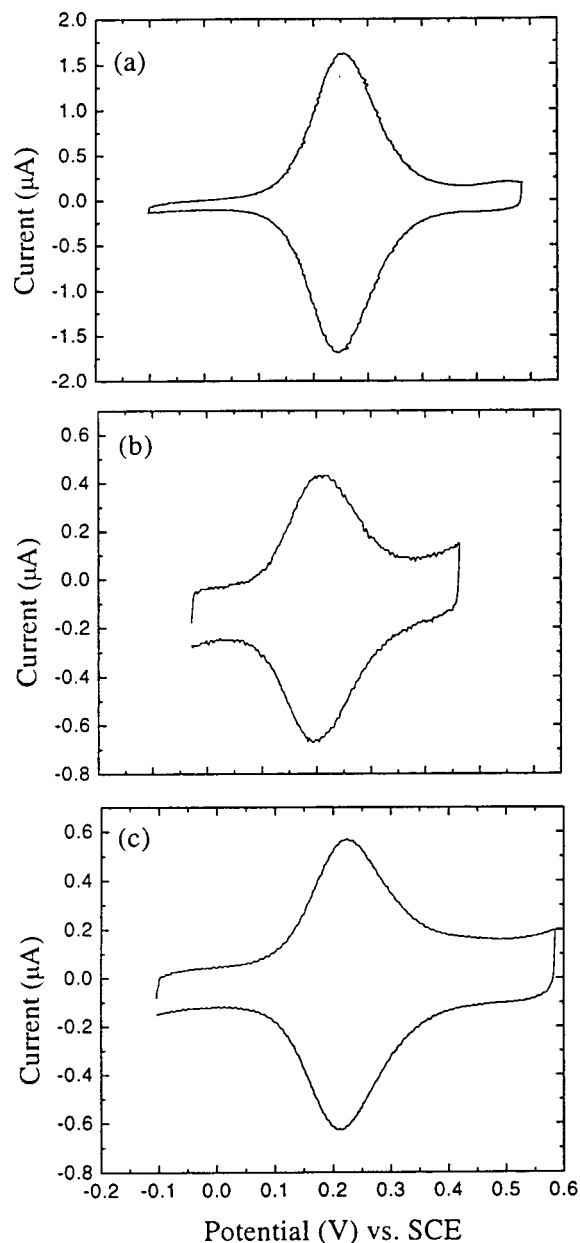


**Figure 2.** CVs of monolayers containing decanethiol and (a) **2a**, (b) **2b**, and (c) **2c**. The scan rate is 100 mV/s.

**Table 2.** Ellipsometric Film Thicknesses for a Representative Set of Mixed Monolayers

electroactive compound	diluent	ellipsometric film thickness (Å)
<b>1b</b>	CH <sub>3</sub> (CH <sub>2</sub> ) <sub>4</sub> SH	6.3 ± 1.2
<b>2b</b>	CH <sub>3</sub> (CH <sub>2</sub> ) <sub>9</sub> SH	13.0 ± 0.6
<b>3a</b>	CH <sub>3</sub> (CH <sub>2</sub> ) <sub>9</sub> SH	13.2 ± 1.1
<b>3a</b>	CH <sub>3</sub> (CH <sub>2</sub> ) <sub>15</sub> SH	21.2 ± 1.3
<b>4</b>	CH <sub>3</sub> (CH <sub>2</sub> ) <sub>15</sub> SH	21.5 ± 0.9

to the length of the alkanethiol diluent (Table 2), a reasonable result considering that the diluent comprises the majority of the monolayer. For the monolayer of **2a** described above, the ellipsometric thickness is 13 Å, which is consistent with the effective dielectric thickness of 11 Å. Furthermore, the similarity of the film's ellipsometric thickness to the thickness of a pure alkanethiol monolayer indicates that the OPV chains have not formed multilayers.

Panels b and c of Figure 2 respectively show CVs of monolayers deposited from solutions of the solubilized OPV

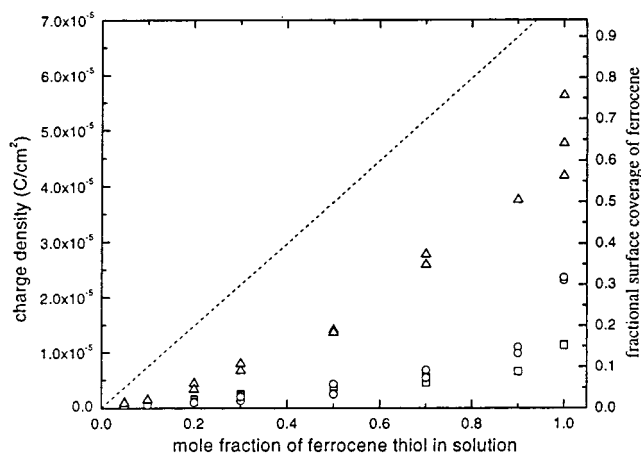


**Figure 3.** Charge density and coverage of the electroactive species (triangles, **2a**; circles, **2b**; squares, **2c**) on the surface as a function of mole fraction in the deposition solution. Decanethiol was used as diluent in all monolayers.

dimers **2b** and **2c** and decanethiol. Cyclic voltammetry and ellipsometry show negligible difference in peak shapes and film thicknesses between the **2a**, **2b**, and **2c** mixed monolayers, suggesting that the presence and position of solubilizing groups on the OPV chain do not prevent the formation of a dense monolayer. The interfacial capacitances and effective dielectric thicknesses of monolayers **2b** and **2c** are  $3.0$  ( $7 \text{ \AA}$ ) and  $3.8 \mu\text{F}/\text{cm}^2$  ( $5 \text{ \AA}$ ), indicating some ion permeation into the monolayer on the CV time scale. Monolayers containing the other ferrocene-terminated OPV methyl thiols show similar CV peak shapes and splittings.

CVs of mixed monolayers deposited from solutions containing the nine ferrocene-terminated OPV methyl thiols with alkanethiol diluents show that the redox peak positions,  $E^\circ$ , are between  $+0.14$  and  $+0.24$  V vs SSCE with no discernible correlation between oligomer length and  $E^\circ$ . There is  $\sim 40$  mV of variability in the value of  $E^\circ$  recorded for the same electroactive thiol. Solubilized oligomers **1b** and **2b** have  $E^\circ$ 's  $25$ – $50$  mV lower than their unsolubilized counterparts **1a** and **2a**, probably because the diethoxy solubilizing groups donate electron density to the conjugated chain making the pendant ferrocene easier to oxidize. Likewise, the trimer with two sets of solubilizing groups, **3b**, has an  $E^\circ$  lower than the  $E^\circ$  for the singly solubilized trimer **3a** (Scheme 4). The  $E^\circ$ 's of ferrocene-terminated OPV methyl thiols absorbed on gold are  $\sim 200$  mV lower than the  $E_{1/2}$ 's of the ferrocene-terminated OPV methyl thioacetates in acetonitrile. It is probable that the  $E^\circ$ 's of the absorbed thiols are lower than the  $E_{1/2}$ 's of the corresponding thioacetates in solution because the electrochemical environments of the two systems are different: the thioacetates are analyzed in  $1 \text{ M}$  tetrabutylammonium hexafluorophosphate in acetonitrile, a solution with a lower dielectric constant than  $1 \text{ M}$  aqueous perchloric acid in which the absorbed thiols are oxidized.

Figure 3 shows charge densities calculated from CVs of **2a**, **2b**, and **2c** as a function of the mole fraction of ferrocenethiol in solution. The coverage, expressed as a fraction of the density of the  $\sqrt{3} \times \sqrt{3} R$   $30^\circ$  alkanethiol monolayer on Au(111), is indicated on the right-hand axis. The coverages of **2b** and **2c** are similar. That is, whether the ethoxy solubilizing groups are positioned on the thiol end or the ferrocene end of the electroactive adsorbate does not appear to affect its competition with the alkanethiol adsorbate in the self-assembly process. However, in the absence of 3,5-diethoxy groups, surface coverages are higher. Either the lower solubility of **2a** in the

deposition solvent as compared to **2b** or **2c** causes higher surface coverages or the bulky diethoxy groups on **2b** and **2c** reduce the packing energy of the OPV adsorbates relative to **2a**. As expected, the longer oligomers show higher ferrocene surface coverages than the shorter oligomers at the same mole fraction in solution because of the lower solubility of the longer oligomers. For example, comparing oligomers having the same number of solubilizing groups but different lengths, a solution of  $20 \text{ mol } \%$  **3a** and  $80 \text{ mol } \%$  decanethiol exhibits a fractional surface ferrocene of  $0.042$ , which is 3 times as much as exhibited for **2b** ( $0.014$ ) at the same solution concentration of ferrocene and with the same diluent.

Potential-step chronoamperometry can be used to determine the rate of electron transfer between an electroactive species and a planar macroscopic electrode through a monolayer film if the electron-transfer rate constant is  $\sim 10^4 \text{ s}^{-1}$  or slower.<sup>23</sup> For rate measurements faster than  $10^4 \text{ s}^{-1}$ , the decay of the current transients is limited by uncompensated solution resistance.<sup>24</sup> Chronoamperometric measurements on mixed monolayers containing the five oligomer lengths of ferrocene-terminated OPV methyl thiols have shown no evidence of current transients slow enough to allow measurement of the electron-transfer rate constants.

Electron-transfer rate measurements have been made on this system with a technique that can probe faster rates, the indirect laser-induced temperature jump method (a potentiometric method).<sup>25</sup> The measured standard rate constants for electron transfer are all greater than  $5 \times 10^5 \text{ s}^{-1}$  for the five oligomer chain lengths and have been interpreted as indicating electron tunneling time constants in the activated complexes of less than  $200 \text{ ps}$ . As a point of comparison, extrapolation of the distance-dependent rate constants reported for ferrocene ester-linked alkanethiols<sup>6</sup> to the same length as **5** gives a standard constant of  $4 \times 10^{-5} \text{ s}^{-1}$ , 10 orders of magnitude slower than **5**. This extraordinary contrast in the rate of electron transfer is due to different tunneling rates through saturated versus well-conjugated insulating molecular bridges and should be of use in molecular electronics.

In summary, we have synthesized a new class of ferrocene-terminated adsorbates, ferrocene oligo(phenylenevinylene) methyl thiols that, with and without solubilizing 3,5-diethoxy groups, form well-ordered self-assembled monolayers on gold which behave thermodynamically similarly to ferrocene ester-linked alkane thiols but have much faster electron-transfer kinetics. The orthogonal strategy presented for the synthesis of these OPV bridges should permit further extension of the OPV chain to greater lengths with retention of sufficient solubility. Syntheses of ferrocene-terminated OPV hexamer and heptamer methyl thiols are in progress. Because the synthesis is asymmetric, the bridge ends can be individually modified to immobilize OPV on surfaces other than gold and to transfer electrons to electroactive groups other than ferrocene. For instance, in work that will be presented elsewhere, we have synthesized pyridine-terminated OPV methyl thiols that can connect transition metal centers to gold electrodes and rapidly transport electrons between them.

## Experimental Section

**Thioacetate Characterization.** Listed below are the characterization data for the protected ferrocene OPV methyl thioacetates from which the thiols are formed. This is the form in which the compounds are

(23) Chidsey, C. E. D. *Science* **1991**, *251*, 919.

(24) Sachs, S. B.; Chidsey, C. E. D. Private communication.

(25) Sikes, H. D.; Smalley, J. F.; Dudek, S. P.; Cook, A. R.; Newton, M. D.; Chidsey, C. E. D.; Feldberg, S. W. *Science* **2001**, *291*, 1519.

stored because thioacetate-protected oligomers are more stable than their corresponding thiols. As needed to form self-assembled monolayers, the thioacetates are deprotected in small quantities with LiAlH<sub>4</sub> as described in the Supporting Information and deposited onto gold substrates immediately.

**4-((E)-2-Ferrocenylvinyl)benzyl thioacetate (thioacetate of 1a):** <sup>1</sup>H NMR (400 MHz, CDCl<sub>3</sub>, ppm) δ 2.36 (s, SCOCH<sub>3</sub>, 3 H), 4.11 (s, benzyl, 2 H), 4.13 (s, Fc, 5 H), 4.28 (d, Fc, *J* = 1.68 Hz, 2 H), 4.45 (d, Fc, *J* = 1.68 Hz, 2 H), 6.67 (d, vinyl, *J* = 16.0 Hz, 1 H), 6.86 (d, vinyl, *J* = 16.1 Hz, 1 H), 7.25 (d, aromatic, *J* = 8.5 Hz, 2 H), 7.37 (d, aromatic, *J* = 8.1 Hz, 2 H); ES-MS *m/e* 376. Anal. Calcd for C<sub>21</sub>H<sub>20</sub>OFeS: C, 66.85; H, 5.61. Found: C, 67.08; H, 5.53.

**4-((E)-2-Ferrocenylvinyl)-3,5-diethoxybenzyl thioacetate (thioacetate of 1b):** <sup>1</sup>H NMR (400 MHz, CDCl<sub>3</sub>, ppm) δ 1.48 (t, OCH<sub>2</sub>CH<sub>3</sub>, *J* = 6.8 Hz, 6 H), 2.35 (s, SCOCH<sub>3</sub>, 3 H), 4.05 (s, benzyl, 2 H), 4.07 (q, OCH<sub>2</sub>CH<sub>3</sub>, *J* = 6.8 Hz, 4 H), 4.12 (s, Fc, 5 H), 4.23 (t, Fc, *J* = 1.8 Hz, 2 H), 4.44 (t, Fc, *J* = 1.8 Hz, 2 H), 6.47 (s, aromatic, 2 H), 6.99 (d, vinyl, *J* = 16.5 Hz, 1 H), 7.29 (d, vinyl, *J* = 16.5 Hz, 1 H); ES-MS *m/e* 464. Anal. Calcd for C<sub>25</sub>H<sub>28</sub>O<sub>3</sub>FeS: C, 64.66; H, 6.08. Found: C, 64.89; H, 6.02.

**4-[(E)-2-(4-((E)-2-Ferrocenylvinyl)phenyl)vinyl]benzyl thioacetate (thioacetate of 2a):** <sup>1</sup>H NMR (400 MHz, CDCl<sub>3</sub>, ppm) δ 2.36 (s, SCOCH<sub>3</sub>, 3 H), 4.13 (s, benzyl, 2 H), 4.14 (s, Fc, 5 H), 4.30 (s, Fc, 2 H), 4.47 (s, Fc, 2 H), 6.69 (d, vinyl, *J* = 16.2 Hz, 1 H), 6.89 (d, vinyl, *J* = 16.2 Hz, 1 H), 7.27 (d, aromatic, *J* = 8.2 Hz, 2 H), 7.41 (d, aromatic, *J* = 8.2 Hz, 2 H), 7.45 (d, aromatic, *J* = 7.9 Hz, 2 H), 7.47 (d, aromatic, *J* = 7.9, 2 H); MALDI-MS *m/e* 478. Anal. Calcd for C<sub>29</sub>H<sub>26</sub>OSFe: C, 72.80; H, 5.48. Found: C, 72.61; H, 5.36.

**4-[(E)-2-(4-((E)-2-Ferrocenylvinyl)phenyl)vinyl]-3,5-diethoxybenzyl thioacetate (thioacetate of 2b):** <sup>1</sup>H NMR (400 MHz, CDCl<sub>3</sub>, ppm) δ 1.50 (t, OCH<sub>2</sub>CH<sub>3</sub>, *J* = 7.0 Hz, 6 H), 2.36 (s, SCOCH<sub>3</sub>, 3 H), 4.10 (q, OCH<sub>2</sub>CH<sub>3</sub>, *J* = 7.0 Hz, 4 H), 4.11 (s, benzyl, 2 H), 4.14 (s, Fc, 5 H), 4.28 (t, Fc, *J* = 1.8 Hz, 2 H), 4.47 (t, Fc, *J* = 1.8 Hz, 2 H), 6.49 (s, aromatic, 2 H), 6.69 (d, vinyl, *J* = 16.2 Hz, 1 H), 6.86 (d, vinyl, *J* = 16.0 Hz, 1 H), 7.40 (d, aromatic, *J* = 8.3 Hz, 2 H), 7.46 (d, aromatic, *J* = 7.9 Hz, 2 H), 7.48 (d, vinyl, *J* = 16.8 Hz, 1 H), 7.65 (d, vinyl, *J* = 16.6, 1 H); ES-MS *m/e* 566. Anal. Calcd for C<sub>33</sub>H<sub>34</sub>O<sub>3</sub>FeS: C, 69.96; H, 6.05. Found: C, 70.32; H, 5.85.

**4-[(E)-2-(4-((E)-2-Ferrocenylvinyl)-3,5-diethoxyphenyl)vinyl]-benzyl thioacetate (thioacetate of 2c):** <sup>1</sup>H NMR (400 MHz, CDCl<sub>3</sub>, ppm) δ 1.53 (t, OCH<sub>2</sub>CH<sub>3</sub>, *J* = 7.0 Hz, 6 H), 2.37 (s, SCOCH<sub>3</sub>, 3 H), 4.13 (s, benzyl, 2 H), 4.15 (s, Fc, 5 H), 4.17 (q, OCH<sub>2</sub>CH<sub>3</sub>, *J* = 7.0 Hz, 4 H), 4.26 (t, Fc, *J* = 1.8 Hz, 2 H), 4.47 (t, Fc, *J* = 1.7 Hz, 2 H), 6.70 (s, aromatic, 2 H), 7.02 (s, vinyl, 1 H), 7.03 (s, vinyl, 1 H), 7.06 (d, vinyl, *J* = 16.2 Hz, 1 H), 7.28 (d, aromatic, *J* = 8.1 Hz, 2 H), 7.37 (d, vinyl, *J* = 16.5 Hz, 1 H), 7.45 (d, aromatic, *J* = 8.2 Hz, 2 H); MALDI-MS *m/e* 566. Anal. Calcd for C<sub>33</sub>H<sub>34</sub>O<sub>3</sub>SFe: C, 69.96; H, 6.05. Found: C, 69.81; H, 6.03.

**4-[(E)-2-(4-((E)-2-Ferrocenylvinyl)-3,5-diethoxyphenyl)-vinyl]phenylvinyl]benzyl thioacetate (thioacetate of 3a):** <sup>1</sup>H NMR (400 MHz, CDCl<sub>3</sub>, ppm) δ 1.54 (t, OCH<sub>2</sub>CH<sub>3</sub>, *J* = 7.1 Hz, 6 H), 2.37 (s, SCOCH<sub>3</sub>, 3 H), 4.13 (s, benzyl, 2 H), 4.15 (q, OCH<sub>2</sub>CH<sub>3</sub>, *J* = 7.0 Hz, 4 H), 4.16 (s, Fc, 5 H), 4.27 (s, Fc, 2 H), 4.48 (s, Fc, 2 H), 6.72 (s, aromatic, 2 H), 7.06 (s, vinyl, 2 H), 7.07 (d, vinyl, *J* = 17.2 Hz, 1 H), 7.09 (s, vinyl, 2 H), 7.29 (d, aromatic, *J* = 8.0 Hz, 2 H), 7.38 (d, vinyl, *J* = 16.5 Hz, 1 H), 7.45 (d, aromatic, *J* = 8.2 Hz), 7.51 (s, aromatic, 4 H); ES-MS *m/e* 668. Anal. Calcd for C<sub>41</sub>H<sub>40</sub>O<sub>3</sub>SFe: C, 73.65; H, 6.03. Found: C, 73.43; H, 5.91.

**4-[(E)-2-(4-((E)-2-[4-((E)-2-Ferrocenylvinyl)-3,5-diethoxyphenyl]-vinyl)phenyl)vinyl]-3,5-diethoxybenzyl thioacetate (thioacetate of 3b):** <sup>1</sup>H NMR (400 MHz, CDCl<sub>3</sub>, ppm) δ 1.51 (t, OCH<sub>2</sub>CH<sub>3</sub>, *J* = 7.0 Hz, 6 H), 1.54 (t, OCH<sub>2</sub>CH<sub>3</sub>, *J* = 7.0 Hz, 6 H), 2.37 (s, SCOCH<sub>3</sub>, 3 H), 4.08 (s, benzyl, 2 H), 4.11 (q, OCH<sub>2</sub>CH<sub>3</sub>, *J* = 7.0 Hz, 4 H), 4.15 (s, Fc, 5 H), 4.17 (q, OCH<sub>2</sub>CH<sub>3</sub>, *J* = 7.0 Hz, 4 H), 4.26 (s, Fc, 2 H), 4.48 (s, Fc, 2 H), 6.50 (s, aromatic, 2 H), 6.72 (s, aromatic, 2 H), 7.06 (s, vinyl, 2 H), 7.07 (d, vinyl, *J* = 16.6 Hz, 1 H), 7.38 (d, vinyl, *J* = 16.5 Hz, 1 H), 7.50 (s, aromatic, 4 H), 7.51 (d, vinyl, *J* = 16.5 Hz, 1 H), 7.68 (d, vinyl, *J* = 16.5 Hz, 1 H); MALDI-MS *m/e* 755. Anal. Calcd for C<sub>45</sub>H<sub>48</sub>O<sub>5</sub>SFe: C, 71.42; H, 6.39. Found: C, 71.57; H, 6.41.

**4-[(E)-2-(4-((E)-2-[4-((E)-2-Ferrocenylvinyl)phenyl]-vinyl)-3,5-diethoxyphenyl)vinyl]phenylvinyl]-3,5-diethoxybenzyl thioacetate (thioacetate of 4):** <sup>1</sup>H NMR (400 MHz, CDCl<sub>3</sub>, ppm) δ 1.51 (t, OCH<sub>2</sub>CH<sub>3</sub>, *J* = 7.0 Hz, 6 H), 1.55 (t, OCH<sub>2</sub>CH<sub>3</sub>, *J* = 7.0 Hz, 6 H), 2.37 (s, SCOCH<sub>3</sub>, 3 H), 4.08 (s, benzyl, 2 H), 4.11 (q, OCH<sub>2</sub>CH<sub>3</sub>, *J* = 7.0 Hz, 4 H), 4.15 (s, Fc, 5 H), 4.20 (q, OCH<sub>2</sub>CH<sub>3</sub>, *J* = 7.0 Hz, 4 H), 4.29 (s, Fc, 2 H), 4.48 (s, Fc, 2 H), 6.50 (s, aromatic, 2 H), 6.70 (d, vinyl, *J* = 16.2 Hz, 1 H), 6.73 (s, aromatic, 2 H), 6.88 (d, vinyl, *J* = 16.0 Hz, 1 H), 7.06 (d, vinyl, *J* = 16.2 Hz, 1 H), 7.08 (d, vinyl, *J* = 16.2 Hz, 1 H), 7.41 (d, aromatic, *J* = 8.2 Hz, 2 H), 7.50 (m, vinyl and aromatic, 7 H), 7.56 (d, vinyl, *J* = 16.5 Hz, 1 H), 7.68 (d, vinyl, *J* = 16.7 Hz, 1 H), 7.73 (d, vinyl, *J* = 16.5 Hz, 1 H); MALDI-MS *m/e* 859. Anal. Calcd for C<sub>53</sub>H<sub>54</sub>O<sub>5</sub>SFe: C, 74.12; H, 6.34. Found: C, 73.91; H, 6.50.

**4-((E)-2-[4-((E)-2-[4-((E)-2-[4-((E)-2-Ferrocenylvinyl)-3,5-diethoxyphenyl]vinyl)phenyl]vinyl)-3,5-diethoxyphenyl]vinyl)phenylvinyl]-3,5-diethoxybenzyl thioacetate (thioacetate of 5):** <sup>1</sup>H NMR (400 MHz, CDCl<sub>3</sub>, ppm) δ 1.51 (t, OCH<sub>2</sub>CH<sub>3</sub>, *J* = 6.9 Hz, 6 H), 1.54 (t, OCH<sub>2</sub>CH<sub>3</sub>, *J* = 7.1 Hz, 6 H), 1.56 (t, OCH<sub>2</sub>CH<sub>3</sub>, *J* = 7.0 Hz, 6 H), 2.37 (s, SCOCH<sub>3</sub>, 3 H), 4.08 (s, benzyl, 2 H), 4.11 (q, OCH<sub>2</sub>CH<sub>3</sub>, *J* = 7.0 Hz, 4 H), 4.15 (s, fc, 5 H), 4.18 (q, OCH<sub>2</sub>CH<sub>3</sub>, *J* = 6.9 Hz, 4 H), 4.20 (q, OCH<sub>2</sub>CH<sub>3</sub>, *J* = 7.0 Hz, 4 H), 4.26 (s, fc, 2 H), 4.48 (s, fc, 2 H), 6.50 (s, vinyl, 2H), 6.73 (s, aromatic, 2 H), 6.74 (s, aromatic, 2 H), 7.06 (m, aromatic & vinyl, 5 H), 7.45 (d, vinyl, *J* = 16.3 Hz, 1 H), 7.51 (m, aromatic and vinyl, 9 H), 7.58 (d, vinyl, *J* = 16.7 Hz, 1 H), 7.68 (d, vinyl, *J* = 16.6 Hz, 1 H), 7.75 (d, vinyl, *J* = 16.5 Hz, 1H); MALDI-MS *m/e* 1047. Anal. Calcd for C<sub>65</sub>H<sub>68</sub>O<sub>7</sub>SFe: C, 74.41; H, 6.53. Found: C, 74.61; H, 6.43.

**Monolayer Preparation.**<sup>18</sup> A 200-Å-thick adhesion layer of titanium and a 2000-Å-thick layer of gold were evaporated on a clean silicon wafer. After a 5-s dip in a "piranha" solution (1 volume of H<sub>2</sub>SO<sub>4</sub>/1 volume of 30% H<sub>2</sub>O<sub>2</sub>), the gold substrates were rinsed with water, ethanol, and chloroform. The cleaned substrates were soaked in chloroform solutions containing a total concentration of 0.3 mM thiol composed of the desired ferrocene OPV thiol and the diluent thiol. The samples were removed from the deposition solution after 2 h and rinsed sequentially with chloroform, ethanol, water, ethanol, and chloroform and dried under argon.

**Ellipsometry.** Ellipsometry measurements were performed on a Gaertner Auto-Gain L116B ellipsometer.

**Electrochemical Measurements.**<sup>18</sup> Electrochemical measurements were made in a cell in which a bored-out cone of poly(tetrafluoroethylene) was pressed down against the sample. The electrolyte (1 M HClO<sub>4</sub>), the counter electrode (platinum wire), and the reference electrode (Ag/AgClO<sub>4</sub>) were then placed in the bore. A PAR 273 potentiostat, interfaced to a personal computer and modified to provide smooth potential ramps, was used to record cyclic voltammograms and perform chronoamperometry.

**Acknowledgment.** We acknowledge valuable discussions with John Smalley, Steve Feldberg, and Marshall Newton of Brookhaven National Laboratory. This work was supported by the National Science Foundation and the Office of Technology Licensing at Stanford University. S.P.D. acknowledges support from a NIH Biotechnology Training Grant and H.D.S. acknowledges support from a NSF Graduate Fellowship. S.P.D. thanks Dr. Gerald Dudek at the Mass Spectrometry Facility, Department of Chemistry, Harvard University, for mass spectrometric analyses.

**Supporting Information Available:** Synthesis of ferrocene-terminated OPV methyl thiols and their monomer components. This material is available free of charge via the Internet at <http://pubs.acs.org>.